HHS Public Access

Author manuscript

J Vis Exp. Author manuscript; available in PMC 2024 March 13.

Subcellular Imaging of Neuronal Calcium Handling *In Vivo*

Rachel Doser[*,1], **Kaz M. Knight**[*,1,2], **Ennis Deihl**[1], **Frederic Hoerndli**[1]

[1]Department of Biomedical Sciences, Colorado State University College of Veterinary Medicine and Biomedical Sciences

[2]Cellular and Molecular Biology Graduate Program, Colorado State University College of Veterinary Medicine and Biomedical Sciences

Abstract

Calcium (Ca^{2+}) imaging has been largely used to examine neuronal activity, but it is becoming increasingly clear that subcellular Ca^{2+} handling is a crucial component of intracellular signaling. The visualization of subcellular Ca^{2+} dynamics *in vivo*, where neurons can be studied in their native, intact circuitry, has proven technically challenging in complex nervous systems. The transparency and relatively simple nervous system of the nematode *Caenorhabditis elegans* enable the cell-specific expression and *in vivo* visualization of fluorescent tags and indicators. Among these are fluorescent indicators that have been modified for use in the cytoplasm as well as various subcellular compartments, such as the mitochondria. This protocol enables non-ratiometric Ca^{2+} imaging *in vivo* with a subcellular resolution that permits the analysis of Ca^{2+} dynamics down to the level of individual dendritic spines and mitochondria. Here, two available genetically encoded indicators with different Ca^{2+} affinities are used to demonstrate the use of this protocol for measuring relative Ca^{2+} levels within the cytoplasm or mitochondrial matrix in a single pair of excitatory interneurons (AVA). Together with the genetic manipulations and longitudinal observations possible in *C. elegans*, this imaging protocol may be useful for answering questions regarding how Ca^{2+} handling regulates neuronal function and plasticity.

Introduction

Calcium ions (Ca^{2+}) are highly versatile carriers of information in many cell types. In neurons, Ca^{2+} is responsible for the activity-dependent release of neurotransmitters, the regulation of cytoskeletal motility, the fine-tuning of metabolic processes, as well as many other mechanisms required for proper neuronal maintenance and function[1,2]. To ensure effective intracellular signaling, neurons must maintain low basal Ca^{2+} levels in their cytoplasm[3]. This is accomplished by cooperative Ca^{2+} handling mechanisms, including the uptake of Ca^{2+} into organelles such as the endoplasmic reticulum (ER) and mitochondria. These processes, in addition to the arrangement of Ca^{2+}-permeable ion channels in the

Corresponding Author: Frederic Hoerndli, frederic.hoerndli@colostate.edu.
*These authors contributed equally

A complete version of this article that includes the video component is available at http://dx.doi.org/10.3791/64928.

Disclosures
The authors declare no competing interests.

plasma membrane, result in heterogeneous levels of cytoplasmic Ca^{2+} throughout the neuron.

Ca^{2+} heterogeneity during rest and neuronal activation allows for the diverse, location-specific regulation of Ca^{2+}-dependent mechanisms[1]. One example of the concentration-specific effects of Ca^{2+} is the release of Ca^{2+} from the ER through inositol 1,4,5-trisphosphate ($InsP_3$) receptors. Low Ca^{2+} levels in combination with $InsP_3$ are required for the opening of the receptor's calcium-permeable pore. Alternatively, high Ca^{2+} levels both directly and indirectly inhibit the receptor[4]. The importance of Ca^{2+} homeostasis for proper neuronal function is supported by evidence suggesting that disrupted intracellular Ca^{2+} handling and signaling is an early step in the pathogenesis of neurodegenerative disorders and natural aging[5,6]. Specifically, abnormal Ca^{2+} uptake and release by the ER and mitochondria are linked to the onset of neuronal dysfunction in Alzheimer's disease, Parkinson's disease, and Huntington's disease[6,7].

The study of Ca^{2+} dyshomeostasis during natural aging or neurodegeneration requires the longitudinal observation of Ca^{2+} levels with subcellular resolution in a living, intact organism in which the native cellular architecture (i.e., the arrangement of synapses and distribution of ion channels) is maintained. To this end, this protocol provides guidance on the use of two readily available, genetically encoded Ca^{2+} sensors for recording Ca^{2+} dynamics *in vivo* with high spatial and temporal resolution. The representative results acquired using the described method in *C. elegans* demonstrate how the expression of Ca^{2+} indicators in the cytoplasm or mitochondrial matrix of single neurons can allow for the rapid acquisition of fluorescent images (up to 50 Hz) that illustrate the Ca^{2+} dynamics with the additional capability of discerning the Ca^{2+} levels within single spine-like structures and individual mitochondria.

Protocol

1. Creating transgenic strains

1. Using a cloning method of choice[8,9], clone expression vectors to contain the *Pflp-18* or *Prig-3* promoter (for AVA-specific signal in the ventral nerve cord), followed by the Ca^{2+} indicator of choice, and then a 3' UTR (see the discussion for more information)[10]. A list of plasmids and their sources can be found in Supplemental Table 1.

2. Follow the established protocol for the creation of transgenic strains *via* the microinjection of a DNA mix (<100 ng/μL; see Supplemental Table 1 for the concentrations of each plasmid) containing the Ca^{2+} indicator transgene (~20 ng/μL) and the rescue DNA lin-15^{+} (selection marker) into the gonad of a 1 day old adult *C. elegans*[10] (genotype: *lin-15(n765ts)*; phenotype: multi-vulva)[10,11].

   NOTE. Maintain *lin-15(n765ts)* parents at 15 °C to suppress temperature-sensitive mutation.

3. Maintain the injected parents at 20 °C until the F1 progeny reach adulthood to allow for transgenic selection using the absence of the multi-vulva phenotype.

4. Clonally passage[13] adult F1 progeny that do not have the multi-vulva phenotype as this indicates the expression of the extrachromosomal array containing the Ca^{2+} indicator[11].

5. Assess the expression of the Ca^{2+} indicator in the F2 or F3 progeny that do not have the multi-vulva phenotype by mounting and imaging 1 day old adults as described later in section 3.

   NOTE. A relatively high expression of the indicator is required for the rapid acquisition of images as described here (see the discussion for more detail).

6. Perform experiments on subsequent generations of the transgenic strains with an optimal expression of the Ca^{2+} indicator (see the discussion for more detail), maintaining the strains under standard conditions (20 °C on NGM plates)[12].

2. Optical setup

1. Use a microscope capable of long-term time-lapse imaging.

   NOTE. The representative data were acquired using an inverted spinning disk confocal microscope equipped with 488 nm and 561 nm excitation lasers.

2. Use a low-magnification objective (i.e., 10x/0.40) for the crude localization of the worm.

3. To achieve subcellular resolution, switch to and localize the neurons using a high-magnification objective. NOTE. A 100x/1.40 NA oil objective was used to acquire the representative data in this study.

4. Acquire the images using an ultra-sensitive camera capable of rapid image acquisition (>50 fps).

5. Use a standard emission filter for the Ca^{2+} indicator of choice (i.e., a 525 nm ± 50 nm emission filter for GCaMP6f and mitoGCaMP).

6. Add a Z-drift corrector (ZDC) for the acquisition of image streams longer than 10 s, as the desiccation of the agar pad during the imaging session causes the neurite to drift out of focus within several seconds.

   NOTE. If a microscopy set-up does not allow for ZDC, or if long (>20 min) imaging periods are desired, then apply a border of silicon grease or melted petroleum jelly around the agar pad to slow the desiccation.

3. Preparation of worms for imaging

1. Preparing the agar pads

   1. Make 3 mL of 10% agar by dissolving molecular grade agar in M9[12] in a 13 mm × 100 mm glass culture tube and microwaving for several seconds (see Table of Materials).

      NOTE. Molten agar can be kept on a heat block for up to 1 h or can be made fresh each time agar pads are needed.

2. Place a microscope slide between two additional slides that each have two layers of laboratory tape (see Figure 1A–i).
3. Cut the tip of a 1,000 µL pipette tip (without a filter), and use it to pipette a small drop of agar onto the center coverslip (Figure 1A–i).
4. Flatten the agar by pressing another slide down on top of the agar (Figure 1A–ii).
5. After cooling, cut the agar into a small disc using the opening of a 13 mm × 100 mm glass culture tube (Figure 1A–iii), and then remove the surrounding agar.

2. Preparing the worm-rolling solution

1. Dissolve muscimol powder in M9 to create a 30 mM stock. Separate into 50 µL aliquots, and store at 4 °C.
2. Thaw a new aliquot of 30 mM muscimol every 3–5 days (and store at 20 °C while in use).
3. Dilute a 30 mM muscimol stock in a 1:1 ratio with polystyrene beads to make the rolling solution.

3. Positioning a worm for imaging

1. Place 1.6 µL of the rolling solution onto the center of the agar pad.

   NOTE: The amount of liquid should be adjusted for imaging younger (less) or older animals (more).
2. Using the preferred worm pick (i.e., a glass or platinum wire pick)[13], transfer a worm of the desired age without the multi-vulva phenotype[11] into the rolling solution on the agar pad (Figure 1A–iv). NOTE. The representative data are from 1 day old hermaphrodites (GCaMP6f strain = FJH185; mitoGCaMP strain; FJH597; see Supplemental Table 1), which can be identified by the presence of only one row of eggs. See the discussion for more detail on working with worms of different ages.
3. Wait for ~5 min for the muscimol to reduce the worm movement, and then drop a 22 mm × 22 mm coverslip on top of the agar pad, physically restricting the worm movement.
4. For imaging neurites in the ventral nerve cord, roll the worm into the orientation shown in Figure 1B,C by lightly sliding the coverslip.

   NOTE. To visualize the ventral nerve cord, position the worm with the head upward, and roll the worm until the intestine is on the right side of the proximal portion and the left for the distal portion of the worm (from the viewer's perspective). Invert this orientation (Figure 1C) for imaging neurites in the dorsal nerve cord.

4. Mounting the worm on a microscope

1. Place a drop of immersion oil onto the coverslip before mounting it onto the microscope stage.
2. Find the worm using a low-magnification objective (10x) objective in brightfield.
3. Switch to the 100x objective, and adjust the focus.
4. Locate the AVA neurite using the illumination of the GCaMP or mitoGCaMP with the 488 nm imaging laser.

   NOTE: Use small adjustments to prevent squishing the worm or pulling off the coverslip.

4. Acquisition of high-resolution image streams

1. *In vivo* GCaMP imaging
   1. Set the exposure time to 20 ms.
   2. Adjust the imaging laser and acquisition settings until the basal GCaMP fluorescence is in the mid-range of the camera's dynamic range[14]. Refer to the discussion for suggestions on optimizing the imaging parameters using other microscopy setups. NOTE. For the optical setup used in this study, set the 488 nm imaging laser to the following output settings: laser power = 50% and attenuation = 1. Modify the additional acquisition settings as follows: EM gain = 200 and pre-amplifier gain = 1.
   3. After the AVA neurite is located using the GCaMP fluorescence at 100x magnification, set the ZDC (see Table of Materials) to a range of ±30 μm, and initiate continuous autofocusing. Manually correct the focal plane as needed before imaging.
   4. Acquire a stream of images at 100x magnification. Durations as long as 10 min can be achieved with the setup used in this study.
2. *In vivo* mitoGCaMP imaging
   1. Follow steps 4.1.1–4.1.2 as needed to acquire the basal mitoGCaMP fluorescence in the mid-range for the camera's dynamic range[14].

      NOTE. For the optical set-up used in this study, set the 488 nm imaging laser to the following output settings: laser power = 20% and attenuation = 10. Modify the acquisition settings to the following: EM gain = 100 and pre-amplifier gain = 2.
   2. After the mitochondria in the AVA neurite are located using the mitoGCaMP fluorescence, set the ZDC as described above in step 3.3.
   3. Acquire a stream of images at 100x magnification.

5. Image stream analysis

1. Open the image stream in an appropriate image software for analyzing the pixel values in an image series (see Table of Materials).

2. Using the **Polygon Selection** tool, define the subcellular region of interest (ROI) containing GCaMP or mitoGCaMP.

3. Click on **Analyze > Tools > ROI Manager**. In the ROI Manager, click **Add** and then **More > Multi Measure**. In the Multi Measure window, click **OK** to automatically collect the average, minimum, and maximum pixel intensities of the ROI defined above for each frame of the image stream for further analysis.

   NOTE. It is recommended that the average pixel intensity (F_{avg}) is normalized to the minimum intensity (F_{min}) for each ROI using the ratio F_{avg}/F_{min} to account for fluorescence differences due to positioning in the z-plane. Discard the image streams with worm movement during imaging since this would also affect the fluorescence measurements.

Representative Results

These two protocols enable the rapid acquisition of differential Ca^{2+} levels within the subcellular regions and organelles of individual neurites *in vivo* with high spatial resolution. The first protocol allows for the measurement of cytoplasmic Ca^{2+} with high temporal and spatial resolution. This is demonstrated here using the cell-specific expression of GCaMP6f in the glutamatergic AVA command interneurons[15], whose neurites run the entire length of the ventral nerve cord. The rapid acquisition of GCaMP6f fluorescence (50 Hz) enabled the detection of the directional propagation of Ca^{2+} influx (Figure 2A and Supplemental Video 1). The subcellular quantification of GCaMP6f fluorescence revealed that the onset of Ca^{2+} influx was delayed in a portion of the neurite just 10 μm away (Figure 2B). Additionally, this protocol allowed for several observations of compartmentalized Ca^{2+} and subthreshold Ca^{2+} events. For instance, dendritic spine-like structures found along the AVA neurite were seen to have flashes in GCaMP6f fluorescence that occurred independently of neurite activation and did not lead to a propagation of Ca^{2+} influx (Figure 2C,D and Supplemental Video 2).

The second protocol aimed to rapidly measure the relative Ca^{2+} levels in the individual mitochondria in single neurites. Using a worm strain with AVA-specific expression of the mitochondrial matrix-localized Ca^{2+} indicator mitoGCaMP enabled the rapid detection of changes in mitoGCaMP fluorescence at the level of individual mitochondria within the AVA neurite. This imaging protocol revealed different modes of Ca^{2+} uptake into the mitochondria, at least in this neuron. First, the results shown in Figure 3A provide an example of the synchronous uptake of a relatively large amount of Ca^{2+} into a subset of mitochondria. More specifically, these data revealed that Ca^{2+} uptake into some mitochondria was synchronized (Mito1 and Mito2; Figure 3A,B and Supplemental Video 3), whereas neighboring mitochondria did not appear to take up Ca^{2+} (Mito3; Figure 3A,B). Similarly, subsets of mitochondria were seen to rapidly uptake and release small amounts of Ca^{2+}. This also appeared to be synchronous (Mito1 and Mito3, Figure 3C,D and Supplemental Video 4), but again only for a subset of mitochondria (Mito 2, Figure 3C,D).

Discussion

The first consideration when implementing the method described involves the selection of a Ca^{2+} indicator with ideal characteristics for the given research question. Cytoplasmic Ca^{2+} indicators typically have a high affinity for Ca^{2+}, and the sensitivity of these indicators to Ca^{2+} is inversely related to the kinetics (on/off rate)[16,17]. This means that either Ca^{2+} sensitivity or kinetics will need to be prioritized based on the phenomenon of interest. For subcellular compartments with relatively high basal Ca^{2+} levels, such as the ER, Ca^{2+} indicators with low Ca^{2+} affinity should be considered[18]. To generate recombinant DNA for the cell-specific expression of a Ca^{2+} indicator, the preferred cloning technique should be used to insert a cell-specific promoter[19,20] followed by the Ca^{2+} indicator of choice and a 3' UTR. Relatively high expression levels in the AVA neurons can be achieved by constructing a plasmid with the promoters *Pflp-18* or *Prig-3*, a *let-858*, or *unc-54* 3' UTR and microinjecting this plasmid at 15–25 ng/μL (see Supplemental Table 1).

The successful microinjection of the plasmids containing the Ca^{2+} indicator and *lin-15*$^{+}$ into the gonad of *lin-15(n765ts)* mutant worms will yield an F1 progeny that expresses the Ca^{2+} indicator and are rescued for the multi-vulva phenotype. Only a subset (30%–80%) of the F1 generation will transmit the synthetic DNA to the F2 generation. The expression of the Ca^{2+} indicator should be assessed in the rescued F2 or F3 progeny on plates with <60% transmission of the synthetic DNA by mounting and imaging the fluorescence in 1 day old adults that are rescued for the multi-vulva phenotype. The ideal expression level is determined based on the properties and location of the Ca^{2+} indicator, as well as the biological question. If rapid image acquisition is desired, then relatively high expression is ideal. However, an extremely high expression of Ca^{2+} indicators has been found to cause subcellular mislocalization, as well as non-specific expression in other cells or tissues.

Genetically encoded Ca^{2+} indicators have been widely employed for *in vivo* analyses of Ca^{2+} in *C. elegans*, as well as in other model organisms. Some of these studies have achieved single-cell resolution monitoring of Ca^{2+} levels in the neuronal cell body[21,22,23,24]. Measurements of Ca^{2+} influx in neuronal sub-compartments have been achieved *in vivo* in *C. elegans* as well as vertebrate systems but only by recording the Ca^{2+} indicator activity in an entire neurite[25,26] or populations of dendrites[27]. Although measuring Ca^{2+} activity in neuronal cell bodies and dendrites as a whole is reflective of the cell's spiking activity, it does not allow for the observation of the dynamics of Ca^{2+} influx (i.e., the direction or rate of propagation) or sub-threshold Ca^{2+} transients. Few *in vivo* studies have been able to discern Ca^{2+} handling in neurons to the spatial and temporal resolution demonstrated here. It should be noted that the temporal dynamics of Ca^{2+} influx in most *C. elegans* neurons[28] appears to be slower than in vertebrate neurons[29], so it is likely that this rapid imaging protocol would be insufficient for capturing similar temporal dynamics in vertebrate systems. However, recent advancements in two-photon microscopy allow for the ultra-fast (120 Hz), subcellular imaging of calcium in individual hippocampal dendrites in freely behaving mice[30], which provides promise for achieving similar high-resolution Ca^{2+} imaging in vertebrates.

It is important to note that this non-ratiometric approach to *in vivo* Ca^{2+} imaging requires the use of muscimol, which inhibits the contraction of the body wall muscles, thus limiting the worm movement during imaging[31]. If there is excessive movement during imaging (consistent movement in more than ~20% of worms), a new rolling solution should be made with a newly thawed aliquot of muscimol, and the time for which a worm bathes in the rolling solution prior to rolling should be extended. Muscimol is a GABA receptor agonist, meaning it inhibits GABAergic neurons, including those that provide input to the AVA neurons. Additionally, many excitatory neurons, including AVA, express low levels of GABA receptors, so it is likely that the use of muscimol in this protocol decreases the neuronal activity. However, using this protocol, the overall spontaneous activation of AVA is reduced by only ~29% in the presence of muscimol (unpublished data). The activation of other neurons may be more drastically decreased by muscimol, and this can be tested by substituting muscimol for M9 in the rolling solution and conducting imaging in the neuronal cell body at low magnification[32]. An alternative to using muscimol would be to use a ratiometric Ca^{2+} indicator[33,34], which would allow for fluorescence correction due to worm movement. The downside to this approach is that it requires an optical setup capable of dual-wavelength imaging and limits the ability to use a Ca^{2+} indicator in combination with many other fluorescent tools.

One major limitation of the microscopy system described is the reduction of emitted light by the spinning disc, which results in a loss of information. This system could be modified to allow for increased capture of emitted light by implementing a disc with larger-diameter pin holes. However, this alteration would decrease the axial (z-plane) resolution and increase the background fluorescence. Another possible microscopy setup for this purpose would be the fast-scanning light sheet microscope, which has been improved in recent years to allow for rapid (up to 50 Hz) imaging *in situ* and *in vivo*[35].

Assessing the spatiotemporal dynamics of cytoplasmic and mitochondrial Ca^{2+} will allow for a better understanding of how local Ca^{2+} transients, and even subthreshold events, may trigger calcium-dependent signaling or modulate mitochondrial biology. This subcellular, *in vivo* Ca^{2+} imaging could be particularly useful for the study of synaptic plasticity, activity-dependent changes in neuronal metabolism, and the homeostatic modulation of neuronal excitability. Further investigation of how local, subcellular environments adapt around defined states of neuronal activity (i.e., spatially specific concentrations and lifetime of Ca^{2+}) would provide insight into how Ca^{2+} dyshomeostasis leads to pathogenic changes in neuronal function. The ability to study this in a living, intact organism is especially useful as it enables longitudinal studies that would shed light on how and why Ca^{2+} homeostasis changes with natural aging and disease-related neurodegeneration. Applying this method to study aging and neurodegeneration is somewhat limited to the early biological ages in *C. elegans* (<4 days of adulthood). Indeed, the physical manipulation during mounting and positioning the worms for imaging is difficult after about 5 days of adulthood when the worms become flaccid because of decreased muscle tone and cuticle integrity.

Rapid *in vivo* imaging of the dynamics and subcellular handling of Ca^{2+} will be instrumental in our understanding of how neuronal excitability and intracellular signaling are finely regulated spatially and temporally. This protocol could benefit a broad range of research

and researchers in many areas due to the diversity of Ca^{2+}-dependent processes and their central role in neuronal function. For instance, the application of this method in healthy neurons would provide insight into why elevated cytoplasmic Ca^{2+} during aging occurs in conjunction with impairments in synaptic plasticity, inefficient mitochondrial respiration, as well as other dysfunctions[36,37]. Additionally, this method could be used to investigate the causes of age-associated Ca^{2+} dyshomeostasis[38]. However, the application of this method for questions related to aging and neurodegeneration is somewhat limited to the early stages of aging (<5 days of adulthood)[38]. As mentioned above, the imaging of older adult worms (>5 days of adulthood) is difficult using our rolling method, but advances in *C. elegans* microfluidics show promise for imaging with a similar spatial resolution for up to 12 days of adulthood[39,40].

Supplementary Material

Refer to Web version on PubMed Central for supplementary material.

Acknowledgments

This work was supported by the National Institutes of Health (NIH) (R01- NS115947 awarded to F. Hoerndli). We would also like to thank Dr. Attila Stetak for the pAS1 plasmid.

References

1. Berridge MJ Neuronal calcium signaling. Neuron. 21 (1) 13–26 (1998). [PubMed: 9697848]
2. Brini M, Calì T, Ottolini D, Carafoli E Neuronal calcium signaling: Function and dysfunction. Cellular and Molecular Life Sciences. 71 (15), 2787–2814 (2014). [PubMed: 24442513]
3. Brini M, Calì T, Ottolini D, Carafoli E Intracellular calcium homeostasis and signaling. Metal Ions in Life Sciences. 12, 119–168 (2013). [PubMed: 23595672]
4. Berridge MJ The inositol trisphosphate/calcium signaling pathway in health and disease. Physiological Reviews. 96 (4), 1261–1296 (2016). [PubMed: 27512009]
5. Schrank S, Barrington N, Stutzmann GE Calcium-handling defects and neurodegenerative disease. Cold Spring Harbor Perspectives in Biology. 12 (7), a035212 (2020). [PubMed: 31427373]
6. Pchitskaya E, Popugaeva E, Bezprozvanny I Calcium signaling and molecular mechanisms underlying neurodegenerative diseases. Cell Calcium. 70, 87–94 (2018). [PubMed: 28728834]
7. Jadiya P et al. Impaired mitochondrial calcium efflux contributes to disease progression in models of Alzheimer's disease. Nature Communications. 10 (1), 3885 (2019).
8. Zeiser E, Frøkjær-Jensen C, Jorgensen E, Ahringer J MosSCI and gateway compatible plasmid toolkit for constitutive and inducible expression of transgenes in the *C. elegans* germline. PLoS One. 6 (5), e20082 (2011). [PubMed: 21637852]
9. Zhu B, Cai G, Hall EO, Freeman GJ In-Fusion™ assembly: Seamless engineering of multidomain fusion proteins, modular vectors, and mutations. Biotechniques. 43 (3), 354–359 (2007). [PubMed: 17907578]
10. Evans TC Transformation and Microinjection. WormBook. (2006).
11. Giordano-Santini R, Dupuy D Selectable genetic markers for nematode transgenesis. Cellular and Molecular Life Sciences. 68 (11), 1917–1927 (2011). [PubMed: 21431833]
12. Stiernagle T Maintenance of C. elegans. WormBook. (2006).
13. Stiernagle T Maintenance of C. elegans: Transferring worms grown on NGM plates. WormBook. (2006).
14. Ogama T A beginner's guide to improving image acquisition in fluorescence microscopy. The Biochemist. 42 (6), 22–27 (2020).

15. Mellem JE, Brockie PJ, Madsen DM, Maricq A v. Action potentials contribute to neuronal signaling in *C. elegans*. Nature Neuroscience. 11 (8), 865–867 (2009).
16. Zhang Y et al. Fast and sensitive GCaMP calcium indicators for imaging neural populations. *bioRxiv*. 2021.11.08.467793 (2021).
17. Kerruth S, Coates C, Dürst CD, Oertner TG, Török K The kinetic mechanisms of fast-decay red-fluorescent genetically encoded calcium indicators. Journal of Biological Chemistry. 294 (11), 3934–3946 (2019). [PubMed: 30651353]
18. de Juan-Sanz J et al. Axonal endoplasmic reticulum Ca2+ content controls release probability in CNS nerve terminals. Neuron. 93 (4), 867–881.e6 (2017). [PubMed: 28162809]
19. Bhatla NC elegans. neural network. <http://wormweb.org/neuralnet#c=BAG&m=1> (2014).
20. Fung W, Wexler L, Heiman MG Cell-type-specific promoters for *C. elegans* glia. Journal of Neurogenetics. 34 (3–4), 335–346 (2020). [PubMed: 32696701]
21. Ali F, Kwan AC Interpreting in vivo calcium signals from neuronal cell bodies, axons, and dendrites: a review. Neurophotonics. 7 (1), 011402 (2019). [PubMed: 31372367]
22. Tian L et al. Imaging neural activity in worms, flies and mice with improved GCaMP calcium indicators. Nature Methods. 6 (12), 875–881 (2009). [PubMed: 19898485]
23. Mank M et al. A genetically encoded calcium indicator for chronic in vivo two-photon imaging. Nature Methods. 5 (9), 805–811 (2008). [PubMed: 19160515]
24. Birkner A, Tischbirek CH, Konnerth A Improved deep two-photon calcium imaging in vivo. Cell Calcium. 64, 29–35 (2017). [PubMed: 28027798]
25. Ryan KC, Laboy JT, Norman KR Deregulation of mitochondrial calcium handling due to presenilin loss disrupts redox homeostasis and promotes neuronal dysfunction. Antioxidants. 11 (9), 1642 (2022). [PubMed: 36139715]
26. Yang HH et al. Subcellular imaging of voltage and calcium signals reveals neural processing in vivo. Cell. 166 (1), 245–257 (2016). [PubMed: 27264607]
27. Takahashi N, Oertner TG, Hegemann P, Larkum ME Active cortical dendrites modulate perception. Science. 354 (6319), 1587–1590 (2016). [PubMed: 28008068]
28. Nicoletti M et al. Biophysical modeling of *C. elegans* neurons: Single ion currents and whole-cell dynamics of AWCon and RMD. PLoS One. 14 (7), e0218738 (2019). [PubMed: 31260485]
29. Church PJ, Stanley EF Single L-type calcium channel conductance with physiological levels of calcium in chick ciliary ganglion neurons. The Journal of Physiology. 496 (Pt 1), 59–68 (1996). [PubMed: 8910196]
30. O'Hare JK et al. Compartment-specific tuning of dendritic feature selectivity by intracellular Ca 2+ release. Science. 375 (6586), eabm1670 (2022). [PubMed: 35298275]
31. Mclntire SL, Jorgensen E, Horvitz HR Genes required for GABA function in Caenorhabditis elegans. Nature. 364 (6435), 334–337 (1993). [PubMed: 8332190]
32. Doser RL, Amberg GC, Hoerndli FJ Reactive oxygen species modulate activity-dependent AMPA receptor transport in *C. elegans*. The Journal of Neuroscience. 40 (39), 7405–7420 (2020). [PubMed: 32847966]
33. Wu J et al. A long Stokes shift red fluorescent Ca2+ indicator protein for two-photon and ratiometric imaging. Nature Communications. 5, 5262 (2014).
34. Cho J-H et al. The GCaMP-R family of genetically encoded ratiometric calcium indicators. ACS Chemical Biology. 12 (4), 1066–1074 (2017). [PubMed: 28195691]
35. Smith JJ et al. A light sheet fluorescence microscopy protocol for *Caenorhabditis elegans* larvae and adults. Frontiers in Cell and Developmental Biology. 10, 1012820 (2022). [PubMed: 36274853]
36. Müller M et al. Mitochondria and calcium regulation as basis of neurodegeneration associated with aging. Frontiers in Neuroscience. 12, 470 (2018). [PubMed: 30057523]
37. Nikoletopoulou V, Tavernarakis N Calcium homeostasis in aging neurons. Frontiers in Genetics. 3, 200 (2012). [PubMed: 23060904]
38. Chen C-H., Chen Y-C., Jiang H-C., Chen C-K, Pan C-L. Neuronal aging: Learning from *C. elegans*. Journal of Molecular Signaling. 8 (1), 14 (2013). [PubMed: 24325838]

39. Saberi-Bosari S, Huayta J, San-Miguel A A microfluidic platform for lifelong high-resolution and high throughput imaging of subtle aging phenotypes in C. elegans. Lab on a Chip. 18 (20), 3090–3100 (2018). [PubMed: 30192357]

40. Sridhar N, Fajrial AK, Doser RL, Hoerndli FJ, Ding X Surface acoustic wave microfluidics for repetitive and reversible temporary immobilization of C. elegans. Lab on a Chip. 22 (24), 4882–4893 (2022). [PubMed: 36377422]

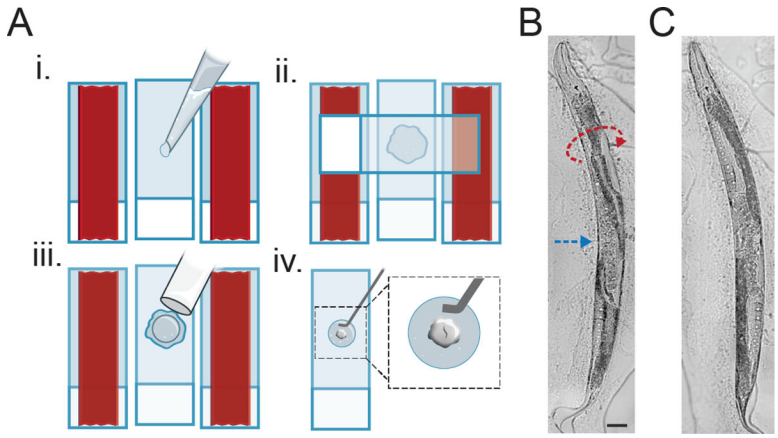

Figure 1: Mounting and rolling *C. elegans* for imaging the ventral nerve cord.
(**A**) An illustration of the steps for preparing the agar pads and picking a single worm into a rolling solution. (**B**) An example of a worm position prior to it being repositioned for imaging. The red arrow indicates the need for a rightward roll of the worm, which can be achieved by sliding the coverslip to the right (blue arrow). Scale bar = 50 μm. (**C**) The correct orientation needed for visualizing the ventral nerve cord. Note: The intestine is on the viewer's right side (using an upright microscope) in the proximal half and is then on the left side in the distal half. Please click here to view a larger version of this figure.

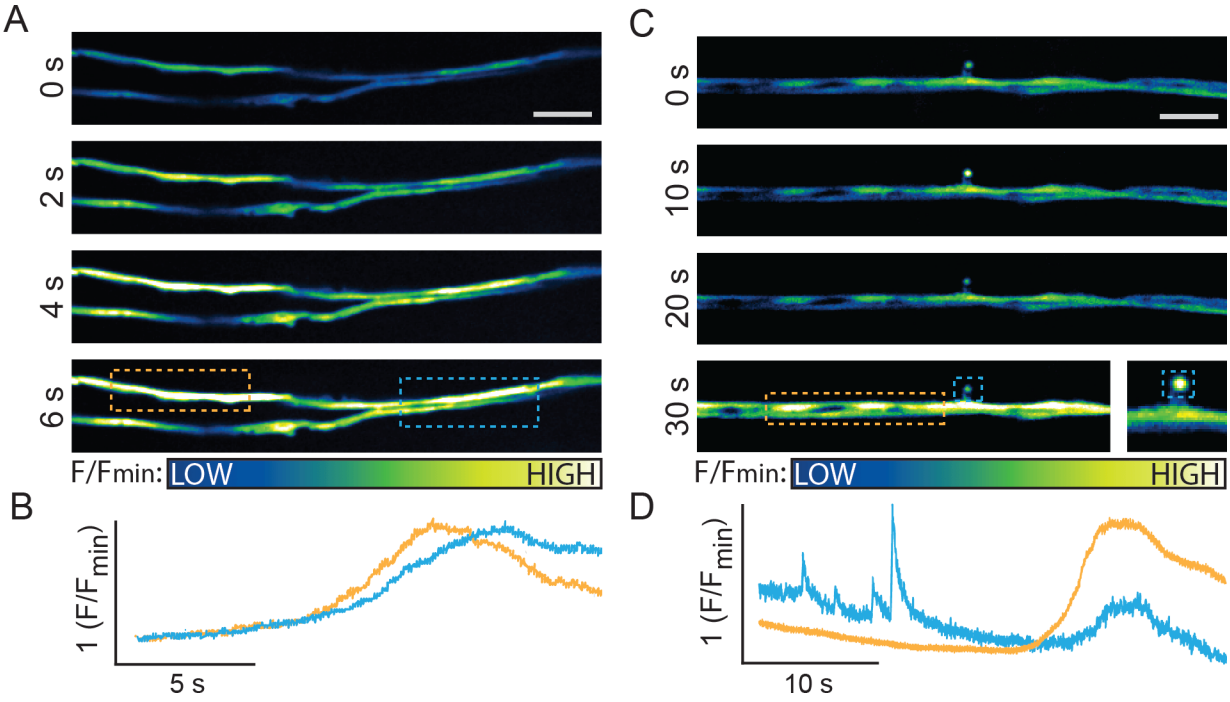

Figure 2: Rapid acquisition of GCaMP6f fluorescence with subcellular resolution in AVA neurite and spine-like structures.

(**A**) Representative images of GCaMP6f fluorescence at the AVAL and AVAR neurite bifurcation. Scale bar = 5 μm. (**B**) Quantification of GCaMP6f fluorescence normalized to the minimum fluorescence (F) for that region (F_{min}) for the proximal (orange) and distal (blue) regions defined in the bottom image in panel A. (**C**) Representative images of GCaMP6f fluorescence at a spine-like projection in the AVA neurite. (**D**) Normalized GCaMP6f fluorescence in the neurite (orange) and the spine-like projection (blue) from the corresponding regions in the bottom image of panel C. Please click here to view a larger version of this figure.

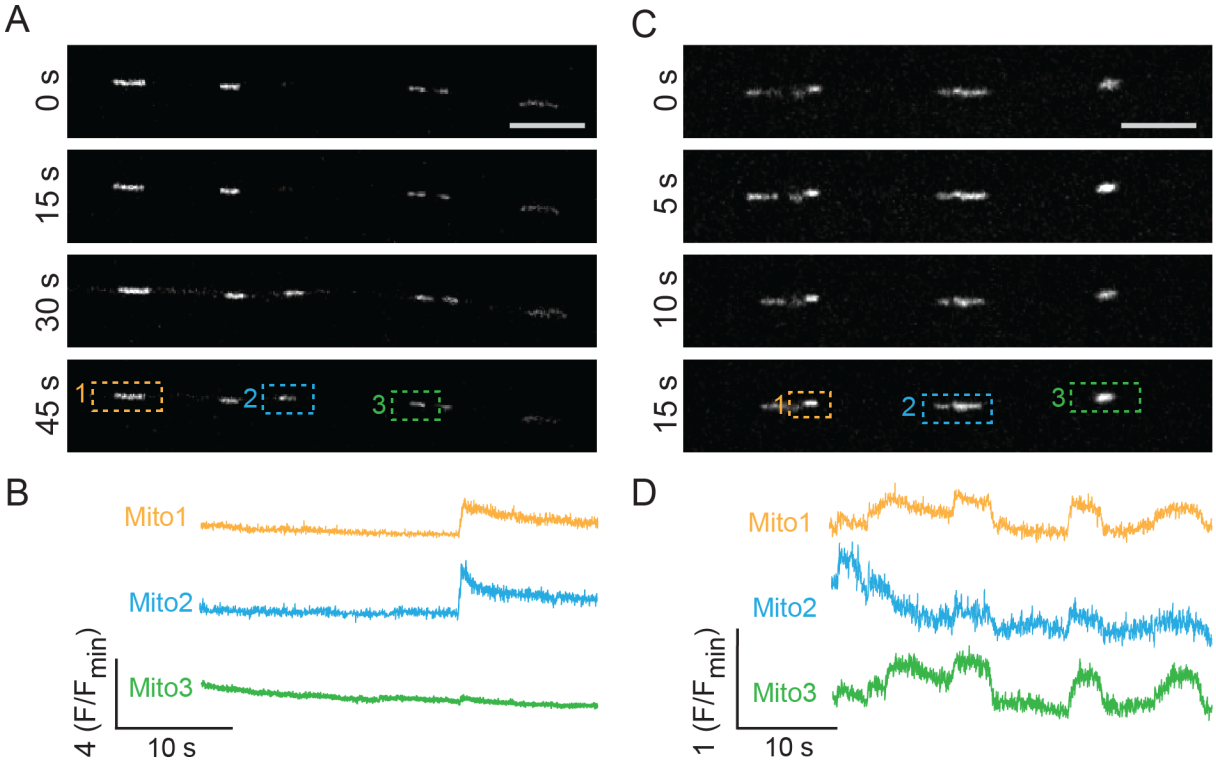

Figure 3. Rapid imaging of calcium uptake into individual mitochondria within the AVA neurite. (**A,C**) Representative images of mitoGCaMP fluorescence over time. Scale bar = 50 μm. (**B**) Traces of normalized GCaMP fluorescence (F/F_{min}) for the corresponding mitochondria shown in the bottom image of panel A. (**D**) F/F_{min} over 40 s of imaging in the regions highlighted in the bottom image in panel C. Please click here to view a larger version of this figure.

Materials

Name	Company	Catalog Number	Comments
100x/1.40 Oil objective	Olympus		UPlanSApo
10x/0.40 Objective	Olympus		UPlanSApo
22 mm × 22 mm Cover glass	VWR	48366–227	
Agarose SFR	VWR	J234–100G	
Beam homogenizer	Andor Technologies		Borealis upgrade to CSU-X1
CleanBench laboratory table	TMC		With vibration control
Disposable culture tubes	VWR	47729–572	13 mm × 100 mm
Environmental chamber	Thermo Scientific	3940	Set to 20 °C
Filter wheel or slider	ASI		For 25 mm diameter filters
FJH 185	Caenorhabditis Genetics Center	FJH 185	Worm strain
FJH 597	Caenorhabditis Genetics Center	FJH 597	Worm strain
GFP bandpass emission filter	Chroma		525 ± 50 nm (25 mm diameter)
ILE laser combiner	Andor Technologies		4 laser lines
ILE solid state 488 nm laser	Andor Technologies		50 mW
ImageJ	National Institutes of Health		Version 1.52a
IX83 Spinning disk confocal microscope	Olympus		With Yokogawa CSU-X1 spinning disc
iXon Ultra EMCCD camera	Andor Technologies		
Low auto-fluorescence immersion oil	Olympus	Z-81226	
MetaMorph	Molecular Devices		Version 7.10.1
Microscope control box	Olympus		IX3-CBH
Muscimol	MP Biomedical / Sigma	02195336-CF	
pAS1	AddGene	194970	Plasmid
pBSKS	Stratagene		
pCT61			Plasmid available from Hoerndli/ Maricq lab upon request
pJM23			Plasmid available from Hoerndli/ Maricq lab upon request
pKK1	AddGene	194969	Plasmid
Polybead microspheres	Polysciences Inc.	00876–15	0.094 μm
Stability chamber	Norlake Scientific	NSRI241WSW/8H	Set to 15 °C
Stage controller	ASI		With filter wheel control
Standard microscope slide	Premiere	9108W-E	75 mm × 25 mm × 1 mm
Touch panel controller	Olympus		I3-TPC
Z-drift corrector	Olympus		IX3-ZDC2